Supplemental Figure 1

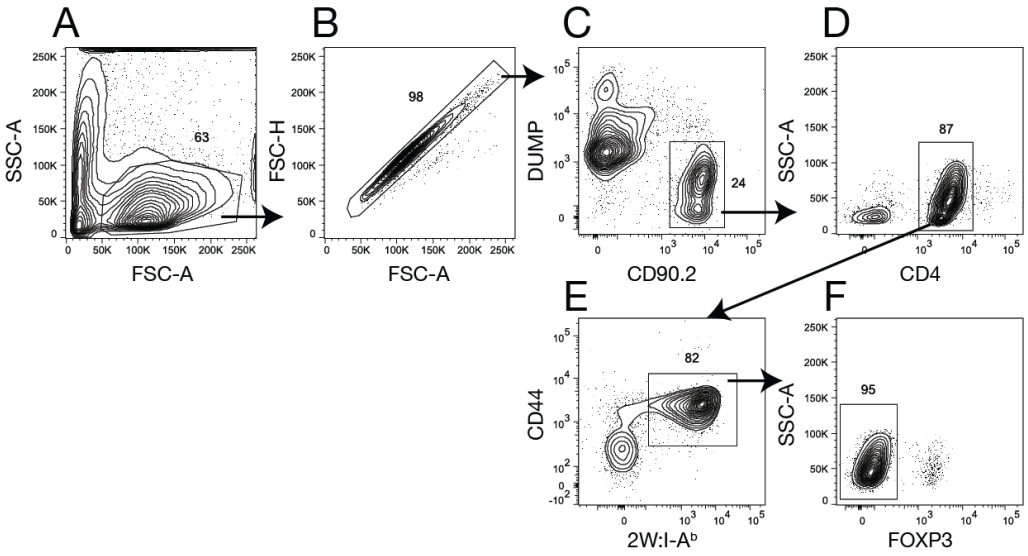

Figure S1 related to Figure 1. Flow cytometry gating strategy for identification of tetramer-binding conventional CD4$^+$ T cells. The figure shows a gating sequence for a spleen and lymph node sample from an IAV-2W-infected B6 mouse after 2W:I-A^b/SA-APC tetramer staining, magnetic enrichment, and staining with fluorophore-conjugated antibodies. The sequence was designed to include cells with light scatter properties of lymphocytes (A), that were singlets (B), non-T lineage-negative CD90$^+$ (C), CD4$^+$ (D), tetramer$^+$ (E), and FOXP3$^-$ (F).

Supplemental Figure 2

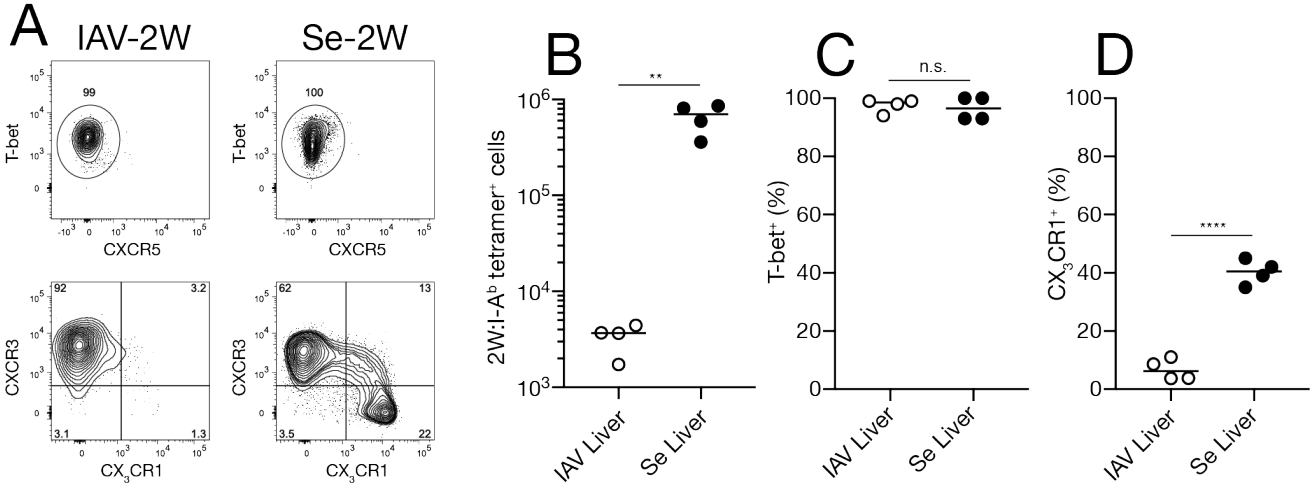

Figure S2 related to Figure 1. Expansion and differentiation of 2W:I-A^b-specific T cells from the liver. (A) Flow cytometry plots of 2W:I-A^b tetramer-binding cells from livers of day 10 IAV-2W or Se-2W-infected mice. (B) Number of 2W:I-A^b tetramer-binding cells from individual mice (n ≥ four from two independent experiments) from the livers of day 10 IAV-2W or Se-2W-infected mice. (C, D) Percent T-bet$^+$ among 2W:I-A^b tetramer-binding cells (C) or percent CX_3CR1^+ cells among T-bet+ 2W:I-A^b tetramer-binding cells (D) from the livers of individual mice (n ≥ four from two independent experiments). Values in B-D were compared using an unpaired Student's t-test ($^{**}p < 0.01$, $^{***}p < 0.001$). Mean values on scatter plots are indicated with a horizontal bar.